Microwave Resonance Relations in Anisotropic Single-Crystal Ferrites*

J. O. ARTMAN†
Lincoln Laboratory, Massachusetts Institute of Technology, Lexington, Massachusetts
(Received July 5, 1956)

The ferromagnetic resonance relations in magnetically anisotropic single-crystal ferrites have been re-examined. Detailed analyses are presented for spherical ferrite specimens possessing first order anisotropy. Generalized nomograms are presented which relate the microwave resonance frequency to the static magnetic field H, the anisotropy parameter K/M, and the static field orientation angle. These curves are derived for both negative and positive anisotropy specimens with **H** lying in a (110) crystal plane.

Below magnetic saturation a simple multi-domain structure is suggested by crystal geometry in which the domains are lamellar in form. The orientations of the magnetizations in these domains are assumed to be of two varieties which alternate in sequence. Equilibrium and resonance results are given for such a configuration when **H** is applied in the [110] direction. Two resonant frequencies are found for a given **H**, depending on whether the microwave field is perpendicular or parallel to **H**. For both positive and negative anisotropy crystals, nomograms are given relating the resonance frequencies to H, K/M, and M. The results depend sensitively on the magnetization M. The nature of the magnetization curve predicted from this structure is discussed.

The angular variation of resonance field and the positions of the secondary resonances found in recent experiments by Tannenwald are in accord with theory.

I. INTRODUCTION

THE ferromagnetic resonance relations in magnetically anisotropic single-crystal ferrites have been re-examined. The basic theory had been considered previously by various authors.[1–4] The results can be derived quite generally; however, the detailed analyses described in this paper were done for spherical ferrite specimens possessing only first order anisotropy. The dc magnetic field in all cases was chosen to lie in a (110) crystal plane. This is the geometry generally selected for microwave measurements since, in this plane, effects in the hard, easy, and intermediate crystal magnetization directions can be examined by orienting the magnetic field appropriately.

Results are given first on the assumption that the specimen exists as a single magnetic domain. Generalized nomograms are presented for both negative and positive anisotropy crystals which relate the microwave resonance frequency to the static magnetic field H, anisotropy parameter K/M, and static field orientation angle ψ. The nature of the gradual alignment of the magnetization **M** to **H** is discussed in detail. Simplified formulas are given for the "quasi-lineup" region in which the angle between **M** and **H** becomes very small. Expressions are also given for the susceptibility tensor components.

Below magnetic saturation a simple multi-domain structure is suggested by crystal geometry in which the domains are assumed to be lamellar in form. The orientations of the magnetizations in these domains are assumed to be of two varieties, disposed in an alternating sequence.[5] The treatment of such a configuration is simplest when **H** is applied along a [110] direction.

Following the methods of Smit and Beljers[2] the multi-domain structure is shown to have *two* resonant frequencies, depending on whether the microwave magnetic field is oriented perpendicular or parallel to **H**. Nomograms are given for both positive and negative anisotropy crystals which relate the resonance frequencies to H, K/M, and M. The resonances predicted from this multi-domain structure are found to depend sensitively on M. Further details of the multi-domain analysis are given in the Appendix. The magnetization curve predicted from this structure is also derived.

The data from some recent experiments are compared with the theory.

II. CONDITIONS FOR EQUILIBRIUM AND RESONANCE—SINGLE-DOMAIN CRYSTALS

In order to demonstrate conveniently ferrite properties in microwave resonance experiments, a standard crystal and field arrangement has become customary; results are given specifically for this geometry but can be derived readily for other cases. The crystal, in the form of a sphere, is mounted on a rotatable post with a [110] crystal axis parallel to the axis of rotation. The microwave and dc magnetic fields are perpendicular to each other and lie in the (110) plane normal to the axis of rotation (see Fig. 1).

* The research reported in this document was supported jointly by the U. S. Army, U. S. Navy, and U. S. Air Force under contract with the Massachusetts Institute of Technology.

† Presently at Gordon McKay Laboratory, Harvard University, Cambridge, Massachusetts.

[1] H. J. Zeiger, Lincoln Laboratory (private communication).

[2] J. Smit and H. G. Beljers, Philips Research Repts. **10**, 113 (1955).

[3] H. Suhl, Phys. Rev. **97**, 555 (1955).

[4] Derivations similar in some respects to references 1 through 3 had been given for antiferromagnetic resonance by C. J. Gorter and J. Haantjes, Physica **18**, 285 (1952), J. Ubbink, Phys. Rev. **86**, 567 (1952), T. Nagamiya, Progr. Theoret. Phys. (Japan) **6**, 350 (1951), and K. Yosida, Progr. Theoret. Phys. (Japan) **7**, 25 (1952).

[5] The structure is similar to that used by Smit and Beljers[2] to explain ferromagnetic resonance effects in uniaxial crystals.

The directions of the [010], [001], and [100] crystal axes define the triad $(\hat{x},\hat{y},\hat{z})$. The dc magnetic field **H** is applied in the (110) plane that passes through the $\hat{z}$ axis and makes an angle ψ with the $\hat{z}$ axis. See Fig. 2.[6] The magnetization **M** is inclined at the angle θ to the $\hat{z}$ axis. The projection of **M** on the x-y plane is inclined at the angle ϕ with respect to $\hat{x}$.

The total energy per unit volume is, considering magnetostatic and anisotropy contributions only,

$$\tfrac{1}{4}K_1[\sin^2(2\theta)+\sin^4\theta\sin^2(2\phi)] - MH[\cos\theta\cos\psi+\sin\theta\sin\psi\sin(\tfrac{1}{4}\pi+\phi)]+\tfrac{2}{3}\pi M^2. \quad (1)$$

The equilibrium point is found from the requirement that the net torque on **M** be zero. This yields the equations:

$$\begin{aligned}\partial E_A/\partial\phi &= -MH\sin\psi\sin(\phi-\tfrac{1}{4}\pi)\sin\theta,\\ \partial E_A/\partial\theta &= MH[\sin\psi\sin(\tfrac{1}{4}\pi+\phi)\cos\theta-\cos\psi\sin\theta],\end{aligned} \quad (2)$$

where

$$E_A=\tfrac{1}{4}K_1[\sin^2(2\theta)+\sin^4\theta\sin^2(2\phi)].$$

To evaluate the ferromagnetic resonant frequency ω_H and the susceptibility tensor components, departure of **M** from equilibrium is considered. Neglecting damping effects, ω_H is given by

$$\omega_H=\frac{1}{M\sin\theta}\{[\gamma MH\cos\psi\cos\theta +\gamma MH\sin\psi\sin(\tfrac{1}{4}\pi+\phi)\sin\theta+\gamma E_{A\theta\theta}] \times[\gamma MH\sin\psi\sin(\tfrac{1}{4}\pi+\phi)\sin\theta+\gamma E_{A\phi\phi}] -[\gamma MH\sin\psi\sin(\tfrac{1}{4}\pi-\phi)\cos\theta+\gamma E_{A\phi\theta}]^2\}^{\frac{1}{2}}, \quad (3)$$

where γ is the gyromagnetic ratio and $E_{A\theta\phi}=\partial^2E_A/\partial\theta\partial\phi$, etc.

Instances occur in which the point of zero torque is not stable. In such cases the expression inside the square brackets (shown above) is negative. Also, as will be discussed below, more than one stable equilibrium point may exist for given H and ψ values. The proper choice would follow from the requirement that the total energy given in Eq. (1) be minimal.

A susceptibility tensor χ may be defined, relating the magnetization to the applied *external* microwave field. This is not a true susceptibility but, nevertheless, still is a convenient way of expressing the ferrite properties. Axes (1,2,3) are chosen: "1," perpendicular to the plane formed by **M** and the [100] direction; "2," normal to **M** and lying in the **M**−[100] plane; "3," parallel to **M**. With reference to this coordinate system, the tensor is:

$$\chi=\begin{bmatrix}\chi_{11} & -j\kappa_{12} & 0\\ j\kappa_{21} & \chi_{22} & 0\\ 0 & 0 & \chi_{33}\end{bmatrix}, \quad (4)$$

[6] Strictly speaking, the (110) plane and [110] direction shown in this diagram are an (01$\bar{1}$) plane and [011] direction, respectively. The somewhat incorrect notation will, however, be used throughout this paper.

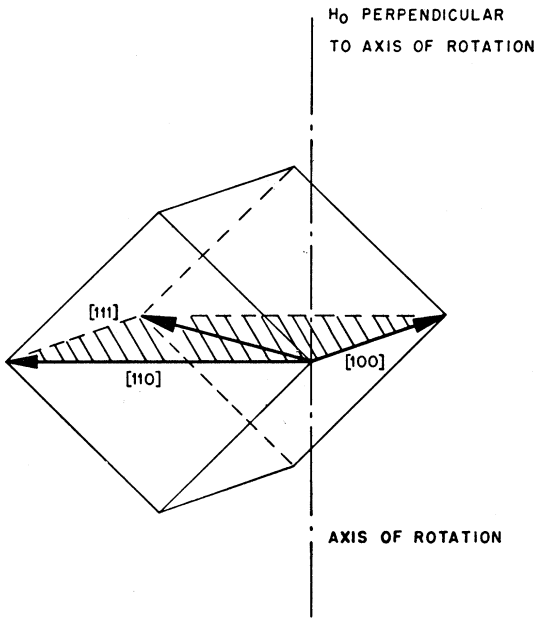

FIG. 1. Principal axes in a cubic crystal.

where the elements are

$$\begin{aligned}\chi_{11}&=\frac{4\pi\gamma M}{D}\left(\gamma H_z\cos\theta+\gamma H_r\sin\theta+\frac{\gamma E_{A\theta\theta}}{M}\right),\\ \chi_{22}&=\frac{4\pi\gamma M}{D}\left(\frac{\gamma H_r}{\sin\theta}+\frac{\gamma E_{A\phi\phi}}{M\sin^2\theta}\right),\\ j\kappa_{21}&=\frac{4\pi\gamma M}{D}\left(j\omega+\frac{1}{T}+\gamma H_q\cot\theta+\frac{\gamma E_{A\theta\phi}}{M\sin\theta}\right),\\ j\kappa_{12}&=\frac{4\pi\gamma M}{D}\left(j\omega+\frac{1}{T}-\gamma H_q\cot\theta-\frac{\gamma E_{A\theta\phi}}{M\sin\theta}\right),\\ \chi_{33}&=0,\end{aligned} \quad (5)$$

with D equal to $\omega_H^2-\omega^2+1/T^2+j(2\omega/T)$, ω_H given by

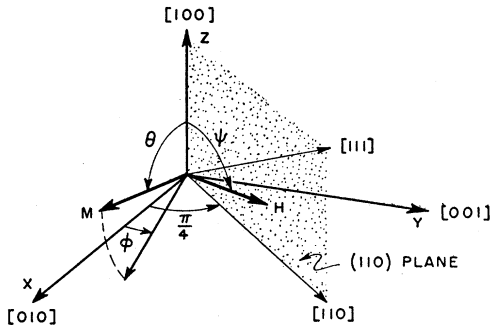

FIG. 2. Spatial configuration of **M** and **H**.

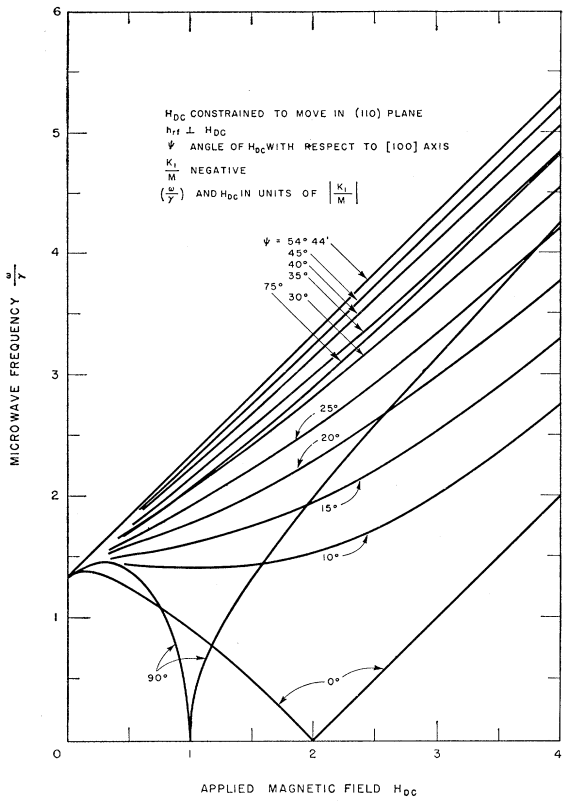

FIG. 3. Single-domain resonance relations in cubic crystal; K_1/M negative.

Eq. (3), and

$$H_q = H \sin\psi \sin(\phi - \tfrac{1}{4}\pi),$$
$$H_r = H \sin\psi \sin(\tfrac{1}{4}\pi + \phi), \qquad (6)$$
$$H_z = H \cos\psi.$$

The properties of the normal modes of oscillation of the ferrite follow immediately from diagonalization of this tensor.

A. Negative Anisotropy Crystals

From energy considerations it is evident that **M** lies in the given (110) plane. The formulas, Eqs. (2) and (3), apply with $\phi = \pi/4$. Normalized curves relating $(\omega/\gamma)/|K_1/M|$ to $H/|K_1/M|$ for various values of ψ are given in Fig. 3.[7] These curves converge to $(\omega/\gamma)/|K_1/M| = 4/3$ for $H = 0$. Values of ψ in the three principal crystal directions 0, 54°44′, 90° must be considered specially.

ψ equal to 54°44′ corresponds to the [111] line, an easy anisotropy axis. θ always equals ψ in this direction and the resonance condition is simply $\omega_H/\gamma = H + (4/3)|K_1/M|$.

Initially **M** is not lined up with **H** for the $\psi = 0°$ ([100] direction) and $\psi = 90°$ ([110] direction) curves. **M** is gradually pulled into alignment as **H** is increased from zero. The ω/γ curves bend toward the $\omega/\gamma = 0$ line which is reached when $H/|K_1/M| = 2$ and $H/|K_1/M| = 1$, respectively; at these points θ equals ψ. **M** remains parallel to **H** along the right-hand portions of these curves for which the resonance conditions are

$$\omega_H/\gamma = H - 2|K_1/M|,$$
$$\omega_H/\gamma = [(H - |K_1/M|)(H + 2|K_1/M|)]^{\frac{1}{2}},$$

respectively.

For all other ψ values, **M** is gradually pulled in toward **H** from the [111] direction; the direction of **M** approaching that of **H** asymptotically as H approaches infinity. The ω/γ curves tend upward as shown. In some instances for a given ψ, a particular ω/γ may correspond to several values of H. In an experiment in which the microwave frequency is fixed and the dc magnetic field slowly varied, several ferrite resonances would be observed.

B. Positive Anisotropy Crystals

The curves relating $(\omega/\gamma)/(K_1/M)$ to $H/(K_1/M)$ for various values of ψ are given in Fig. 4. These curves converge to $(\omega/\gamma)/(K_1/M) = 2$ for $H = 0$. For $\psi = 0°$ **M** lies parallel to **H**. This is the [100] direction, an easy anisotropy axis for which the resonance relation is simply $\omega_H/\gamma = H + 2K_1/M$. For values of ψ between 0° and 54°44′, **M** lies in the (110) plane and is tipped in toward H asymptotically from the [100] direction. For values of ψ between 54°44′ and 90°, **M** is drawn in toward **H** from the [010] or [001] direction.[8] These will be termed "skew" orientations. As **H** is increased from zero these skew solutions curve in toward the $(\omega/\gamma) = 0$ line. At the point $\phi = \frac{1}{4}\pi$, corresponding to $(\omega/\gamma) = 0$, **M** has been pulled into the (110) plane. However, **M** is not parallel to **H**. As **H** increases further, **M**, lying in the (110) plane, is asymptotically pulled into alignment with **H**.

The solution for $\psi = 90°$ is a limiting case in which **M** always lies in the (100) plane while "skewly" oriented. At $H/(K_1/M) = 2$, $(\omega/\gamma)/(K_1/M)$ is zero. At this point, $\phi = \frac{1}{4}\pi$ and **M** has become parallel to **H**. **M** then remains parallel to **H** as the field is increased. The right-hand portion of the curve is then obtained, for which the resonance relation is

$$\omega_H/\gamma = [(H + K_1/M)(H - 2K_1/M)]^{\frac{1}{2}}.$$

The solution for $\psi = 54°44'$ is another special case. Three types of single domain solutions are possible, all equivalent to each other and yielding the same ω/γ *vs* H curve. These are: the given (110) plane solution corresponding to **M** being tipped in from the [100] direction; and two skew solutions corresponding to **M** being tipped in from the [010] and [001] directions. As **H** increases

[7] Adapted in part from calculations by P. E. Tannenwald and Marjorie M. Campbell, Lincoln Laboratory, Massachusetts Institute of Technology.

[8] A graphical method for obtaining some of these equilibrium conditions was given by R. M. Bozorth and H. J. Williams, Phys. Rev. **59**, 827 (1941).

from zero, the resonance curve bends toward the $(\omega/\gamma)=0$ line which is reached when $H/(K_1/M)$ is 1.483. The ω/γ solution for **M** parallel to **H** is a straight line inclined at 45° and terminating at $H/(K_1/M)=4/3$. The curves intersect as shown. For all points to the right of $H/(K_1/M)=1.466$, the lineup solution has the lower total energy. At this point, indicated by a dotted line, a jump is made from one curve to the other. The resonance relation for the lineup solution is $\omega_H/\gamma=H-(4/3)(K_1/M)$. As in the negative anisotropy case, multiple ferrite resonances may be observed under appropriate conditions.

III. EQUILIBRIUM AND RESONANCE CONDITIONS WHEN M AND H LIE IN THE (110) PLANE; QUASI-LINEUP CONDITIONS

As discussed in Sec. II, **M** will lie in the (110) plane for negative anisotropy crystals and also for positive anisotropy crystals when sufficiently high dc magnetic fields are applied. When **M** lies in the (110) plane, the azimuth angle ϕ equals $\frac{1}{4}\pi$. The equilibrium conditions, Eq. (2), simplify to

$$\partial E_A/\partial\theta=MH\sin(\psi-\theta). \tag{7}$$

The resonant angular frequency ω_H, Eq. (3), is now

$$\omega_H=\left[\left(\gamma H\frac{\sin\psi}{\sin\theta}+\frac{\gamma E_{A\phi\phi}}{M\sin^2\theta}\right)\times\left(\gamma H\cos(\theta-\psi)+\frac{\gamma E_{A\theta\theta}}{M}\right)\right]^{\frac{1}{2}}. \tag{8}$$

In the limit of large magnetic fields, $H/|K_1/M|\gg 0$, **M** tends to become parallel to **H** and $(\psi-\theta)\equiv\epsilon$ approaches zero. This condition, for which **M** lies in the (110) plane and $|\epsilon|\lesssim 5°$, will be termed "quasi-lineup." **M** can become parallel to **H** only in the three principal crystal directions for which $\partial E_A/\partial\theta=0$. Since $\partial E_A/\partial\theta=K_1\sin\theta\cos\theta(3\cos^2\theta-1)$, these correspond to $\psi=\theta=0°$, 54°44′, and 90°.

Putting θ equal to ψ in Eq. (8) does not yield the proper limiting lineup formula originally derived by Bickford.[9] The correct relation is obtained as follows: to the first order in ϵ the resonance equation is

$$\left(\frac{\omega_H}{\gamma}\right)=\left[\left(H+H\epsilon\cot\theta+\frac{E_{A\phi\phi}}{M\sin^2\theta}\right)\left(H+\frac{E_{A\theta\theta}}{M}\right)\right]^{\frac{1}{2}}.$$

From the equilibrium condition $H\epsilon=(1/M)(\partial E_A/\partial\theta)$. Hence,

$$\left(\frac{\omega_H}{\gamma}\right)=\left[\left(H+\frac{\cot\theta}{M}E_{A\theta}+\frac{E_{A\phi\phi}}{M\sin^2\theta}\right)\left(H+\frac{E_{A\theta\theta}}{M}\right)\right]^{\frac{1}{2}}. \tag{9}$$

This relation between ω_H and θ is equivalent to the relation between ω_H and ψ derived by Bickford. The present ω/γ *vs* ψ plot is not the same as the ω/γ *vs* θ plot since ψ and θ are not necessarily equivalent. These conclusions hold also in the presence of second order anisotropy:

$$E_{2A}=\tfrac{1}{16}K_2[\sin^2(2\phi)\sin^2(2\theta)\sin^2\theta].$$

The more general relation for ϵ is

$$\epsilon=\frac{1}{MH}\sin\theta\cos\theta(3\cos^2\theta-1)\left(K_1+\frac{K_2}{2}\sin^2\theta\right),$$

or

$$\epsilon=\frac{1}{H}\left[F_1(\theta)\frac{K_1}{M}+F_2(\theta)\frac{K_2}{M}\right], \tag{10}$$

where ϵ is now expressed in degrees and

$$F_1=57.296\sin\theta\cos\theta(3\cos^2\theta-1),$$

$$F_2=57.296\sin\theta\cos\theta(3\cos^2\theta-1)\times\tfrac{1}{2}\sin^2\theta.$$

F_1 and F_2 are plotted in Fig. 5.

In Figs. 6 and 7 the resonance nomograms are plotted for very high fields where the lineup formulas apply and for which, in addition, the resonance relation, Eq. (9), can be approximated by

$$\omega_H/\gamma=H+\tfrac{1}{2}\left(\frac{\cot\theta}{M}E_{A\theta}+\frac{E_{A\phi\phi}}{M\sin^2\theta}+\frac{E_{A\theta\theta}}{M}\right). \tag{11}$$

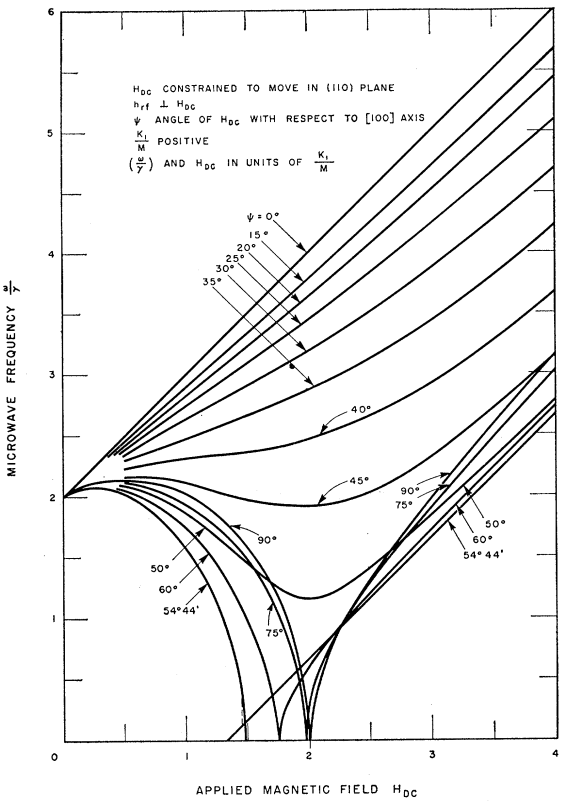

FIG. 4. Single-domain resonance relations in cubic crystal; K_1/M positive.

[9] L. R. Bickford, Jr., Phys. Rev. **78**, 449 (1950).

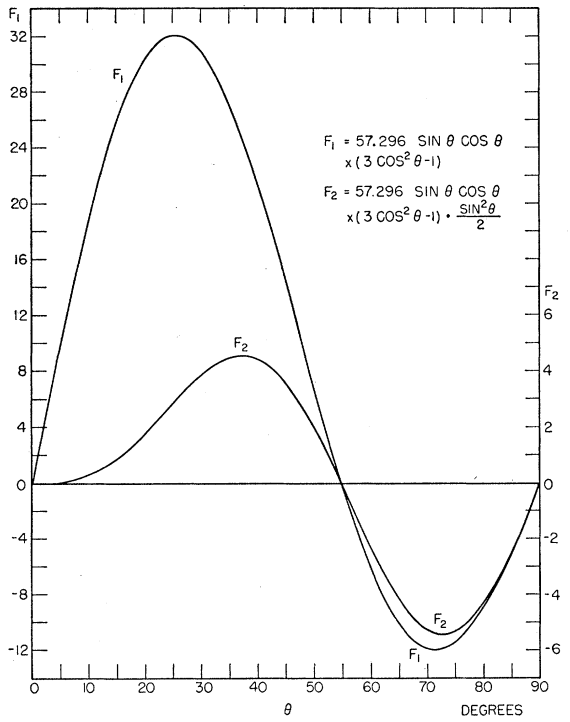

FIG. 5. Tilt angle functions F_1 and F_2.

Substituting for the anisotropy terms,

$$\frac{\omega_H}{\gamma}=H+\frac{K_1}{M}\left(2+\frac{15}{2}\sin^4\theta-10\sin^2\theta\right).$$

Figures 6 and 7 should be compared to the previous Figs. 3 and 4.

The susceptibility tensor [see Eq. (4)] described earlier simplifies greatly under lineup conditions. Equations (5) become

$$\chi_{11}=\frac{4\pi\gamma M}{D}\left(\gamma H+\frac{\gamma E_{A\theta\theta}}{M}\right),$$

$$\chi_{22}=\frac{4\pi\gamma M}{D}\left(\gamma H+\frac{\gamma}{M}\cot\theta E_{A\theta}+\frac{\gamma}{M}\frac{E_{A\phi\phi}}{\sin^2\theta}\right), \quad (12)$$

$$\kappa_{12}=\kappa_{21}=\kappa=\frac{4\pi\gamma M}{D}\left(\omega-\frac{j}{T}\right).$$

As before, D is given by $\omega_H^2-\omega^2+1/T^2+j(2\omega/T)$, where ω_H is now obtained from Eq. (9).

IV. FERROMAGNETIC RESONANCE IN THE PRESENCE OF MAGNETIC DOMAIN STRUCTURE

Resonances which are not predictable by the single-domain analysis curves of Sec. II have been observed experimentally in ferrites.[9–14] These resonances, in many cases, have been presumed to be a consequence of the domain structure existing below magnetic saturation. Effects of this nature in magnetically uniaxial crystals have recently been analyzed by Smit and Beljers.[2] Nagamiya[15] has considered domain structure effects in Fe_3O_4 when the magnetic anisotropy has tetragonal symmetry. Treatment of the multiple-domain structure problem in crystals with cubic symmetry is, in general, very involved. One situation for which a solution can be obtained readily in both negative and positive anisotropy crystals occurs when **H** lies along a [110] direction.

In the analysis that follows, the domains are assumed to be lamellae of two varieties arranged alternately. The lamellae are presumed to be equal in volume. The planes of the lamellae are perpendicular to the dc magnetic field direction. Orientations in which these planes are parallel to the magnetic field direction are shown in the Appendix to be unlikely. The treatment of the equations follows very closely that of Smit and Beljers.

A. Negative Anisotropy Crystals—H in [110] Direction

The two types of domains expected correspond to magnetizations lying in the (110) plane tilted equally with respect to the [110] direction. The domains are, therefore, of types 1 and 2 in which the orientation of **M** is specified by the parameters (θ_1, $\phi_1=\frac{1}{4}\pi$) and ($\theta_2=\pi-\theta_1$, $\phi_2=\frac{1}{4}\pi$), respectively (see Fig. 8). The angle nomenclature corresponds to that used previously.

The total energy per unit volume for this multi-domain structure is:

$$\begin{aligned}E=&\tfrac{1}{8}K_1[\sin^2(2\theta_1)+\sin^4\theta_1\sin^2(2\phi_1)\\&+\sin^2(2\theta_2)+\sin^4\theta_2\sin^2(2\phi_2)]\\&-\tfrac{1}{2}MH[\sin\theta_1\sin(\tfrac{1}{4}\pi+\phi_1)+\sin\theta_2\sin(\tfrac{1}{4}\pi+\phi_2)]\\&+\tfrac{1}{6}\pi M^2[(\cos\theta_1+\cos\theta_2)^2+(\sin\theta_1\sin\phi_1+\sin\theta_2\sin\phi_2)^2\\&+(\sin\theta_1\cos\phi_1+\sin\theta_2\cos\phi_2)^2]\\&+\tfrac{1}{2}\pi M^2[\sin\theta_1\cos(\tfrac{1}{4}\pi-\phi_1)-\sin\theta_2\cos(\tfrac{1}{4}\pi-\phi_2)]^2. \quad (13)\end{aligned}$$

The first term represents the crystal anisotropy energy; the second, the magnetostatic energy; the third, the demagnetization energy for the net magnetization in the spherical sample; and the fourth, the demagnetization energy of poles on the walls of the domains—the domain demagnetizing factor is taken as 4π. The equi-

[10] P. E. Tannenwald, Phys. Rev. **99**, 463 (1955).
[11] P. E. Tannenwald, Phys. Rev. **100**, 1713 (1955).
[12] R. L. White and I. H. Solt, Jr., Hughes Research Laboratory, Culver City, California (private communication).
[13] C. Hubbard, Harvard University (private communication).
[14] A. F. Kip and R. D. Arnold, Phys. Rev. **75**, 1556 (1949), observed similar effects in single crystals of iron.
[15] T. Nagamiya, Progr. Theoret. Phys. (Japan) **10**, 72 (1953).

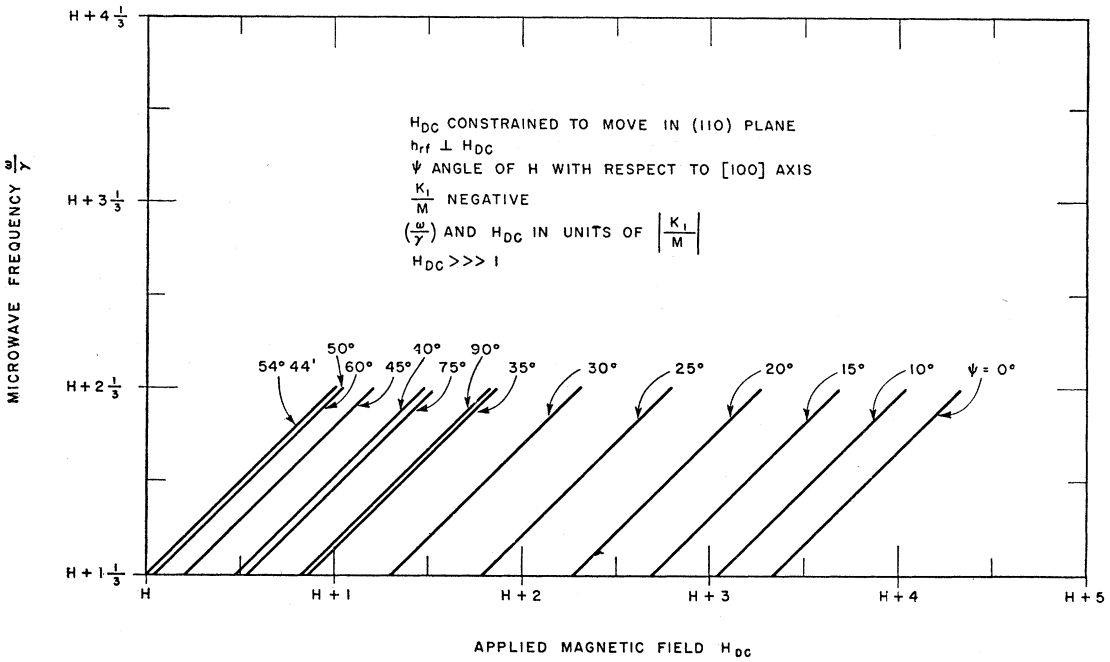

FIG. 6. Resonance relations in cubic crystal at very high magnetic field; K_1/M negative.

librium conditions $\partial E/\partial\theta_1=0$, $\partial E/\partial\theta_2=0$, $\partial E/\partial\phi_1=0$, $\partial E/\partial\phi_2=0$ are, as anticipated, satisfied by $\phi_1=\phi_2=\frac{1}{4}\pi$ and $\theta_2=\pi-\theta_1$. Two resonance conditions are found.

$$\left(\frac{\omega}{\gamma}-M\sin\theta\right)_{\perp}=(AC)^{\frac{1}{2}},\quad \left(\frac{\omega}{\gamma}-M\sin\theta\right)_{\parallel}=(BD)^{\frac{1}{2}},\quad (14)$$

where

$$\begin{aligned} A&=2(E_{\theta_1\theta_1}+E_{\theta_1\theta_2}),\\ B&=2(E_{\theta_1\theta_1}-E_{\theta_1\theta_2}),\\ C&=2(E_{\phi_1\phi_1}+E_{\phi_1\phi_2}),\\ D&=2(E_{\phi_1\phi_1}-E_{\phi_1\phi_2}), \end{aligned}\quad (15)$$

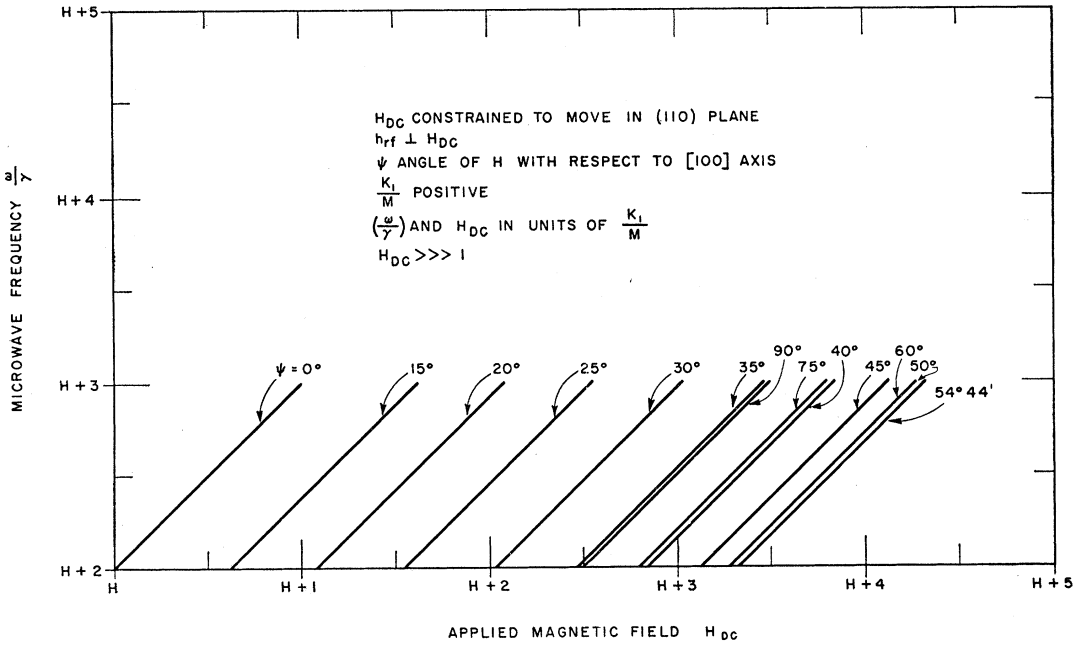

FIG. 7. Resonance relations in cubic crystal at very high magnetic field; K_1/M positive.

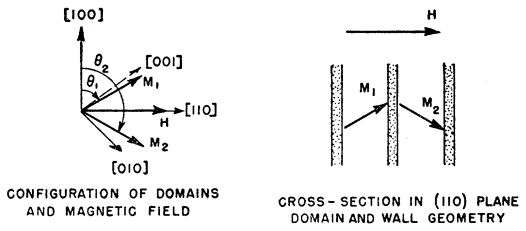

FIG. 8. Multidomain structure in negative anisotropy crystal; **H** in [110] direction.

and

$$\begin{aligned}
E_{\theta_1\theta_1}&=\tfrac{1}{2}K_1[2\cos 4\theta+\sin^2\theta(3-4\sin^2\theta)]\\
&\quad+\tfrac{1}{2}MH\sin\theta+\tfrac{1}{3}\pi M^2\cos 2\theta+\pi M^2\cos^2\theta,\\
E_{\theta_1\theta_2}&=-\tfrac{1}{3}\pi M^2\cos 2\theta+\pi M^2\cos^2\theta,\\
E_{\phi_1\phi_1}&=-K_1\sin^4\theta_1+\tfrac{1}{2}MH\sin\theta\sin\psi-\tfrac{1}{3}\pi M^2\sin^2\theta,\\
E_{\phi_1\phi_2}&=\tfrac{1}{3}\pi M^2\sin^2\theta.
\end{aligned}\tag{16}$$

The $(\omega/\gamma)_\perp$ resonance corresponds to microwave excitation perpendicular to **H** while the $(\omega/\gamma)_\parallel$ resonance corresponds to excitation parallel to **H**.

In Fig. 9, families of the multiple-domain ω/γ *vs* H resonance curves are shown superimposed on the usual single-domain $\psi=90°$ resonance curve (refer to Fig. 3). M, H, and ω_H/γ are expressed in units of $|K_1/M|$. For each value of $M/|K_1/M|$ both the $(\omega/\gamma)_\perp$ and $(\omega/\gamma)_\parallel$ curves are shown.

The energy, equilibrium, and resonance conditions are, if one expresses all quantities in units of $|K_1/M|$,[16]

$$\begin{aligned}
E&=-\tfrac{1}{4}[\sin^2(2\theta)+\sin^4\theta]-H\sin\theta+\tfrac{2}{3}\pi M\sin^2\theta,\\
H&=(3\sin^2\theta-2+(4/3)\pi M)\sin\theta,
\end{aligned}\tag{17}$$

$$\begin{aligned}
(\omega/\gamma)_\perp&=\{[(1-\sin^2\theta)(9\sin^2\theta-2)\\
&\quad+(4/3)\pi M(3-2\sin^2\theta)]\\
&\quad\cdot[(5\sin^2\theta-2)+(4/3)\pi M]\}^{\frac{1}{2}},\\
(\omega/\gamma)_\parallel&=\{[(1-\sin^2\theta)(9\sin^2\theta-2)\\
&\quad+(4/3)\pi M(1-\sin^2\theta)]\\
&\quad\cdot[(5\sin^2\theta-2)]\}^{\frac{1}{2}}.
\end{aligned}\tag{18}$$

For $(4/3)\pi M\geq 2$, equilibria exist for all values of θ, but are not stable below field values less than $(\frac{2}{5})^{\frac{1}{2}}((4/3)\pi M-\frac{4}{5})$ (corresponding to $\theta=\sin^{-1}[(\frac{2}{5})^{\frac{1}{2}}]$) since $(\omega/\gamma)_\parallel$ vanishes at this point. The $(\omega/\gamma)_\parallel$ curves are similar in form to semicircles. $(\omega/\gamma)_\parallel$ vanishes for all values greater than $(4/3)\pi M+1$. This is the point $\theta=\pi/2$, at which the multiple-domain structure ceases to exist. The $(\omega/\gamma)_\perp$ resonance terminates on the single-domain curve at $\theta=\pi/2$, $H=(4/3)\pi M+1$ at the value $(\omega/\gamma)_\perp=\{[(4/3)\pi M][(4/3)\pi M+3]\}^{\frac{1}{2}}$. As H decreases, $(\omega/\gamma)_\perp$ increases, reaching a value of

$$\left[\left(\frac{24}{25}+\frac{11}{5}\cdot\frac{4\pi M}{3}\right)\left(\frac{4\pi M}{3}\right)\right]^{\frac{1}{2}}$$

at $\theta=\sin^{-1}(\frac{2}{5})^{\frac{1}{2}}$, $H=(\frac{2}{5})^{\frac{1}{2}}[(4/3)\pi M-\frac{4}{5}]$. The values of $(\omega/\gamma)_\perp$ in the unstable region below $H=(\frac{2}{5})^{\frac{1}{2}}\times[(4/3)\pi M-\frac{4}{5}]$ are indicated by dashed lines.

When observing $(\omega/\gamma)_\perp$, two resonances may be seen as the dc magnetic field is increased from zero upward. The one at the lower field corresponds to the multiple-domain resonance. The one at the higher field is the usual single-domain resonance. If $(\omega/\gamma)_\perp$ is too large, then only the single-domain resonance will be seen. If $(\omega/\gamma)_\perp$ is too low, then no resonance will be seen.

When investigating $(\omega/\gamma)_\parallel$, two resonances may be seen as H is varied, both due to multiple-domain resonance. If $(\omega/\gamma)_\parallel$ is too high, no resonance will be observed.

As anticipated, the total energy for this multiple-domain structure at a given H is never greater than the energy for the single-domain structure.

A "gross susceptibility tensor" χ_g may be defined in a manner similar to that of Sec. II. The axes of the reference system are as follows: "1," perpendicular to the (110) plane; "2," directed along the $[\bar{1}00]$ axis; "3," parallel to **H**.

The tensor elements [see Eq. (4)] are:

$$\begin{aligned}
\chi_{g11}&=\frac{4\pi M^2A\sin^2\theta}{AC-z^2},\\
\chi_{g22}&=\frac{4\pi M^2C\sin^2\theta}{AC-z^2},\\
\chi_{g33}&=\frac{4\pi M^2D\cos^2\theta}{BD-z^2},\\
\kappa_{g12}&=\kappa_{g21}=\kappa_g=\frac{4\pi M^2z\sin^2\theta}{AC-z^2},
\end{aligned}\tag{19}$$

where A, B, C, and D are defined through Eqs. (15) and (16) and $z=(\omega-j/T)M\sin\theta/\gamma$.

B. Positive Anisotropy Crystals—H in [110] Direction

The analysis is quite similar to that of the negative anisotropy case. Two types of domains are postulated, corresponding to magnetizations lying in the (100) plane tilted equally with respect to the [110] direction. The orientation of the magnetizations in these domains is specified by the angular parameters $(\theta_1=\frac{1}{2}\pi, \phi_1)$ and $(\theta_2=\frac{1}{2}\pi, \phi_2=\frac{1}{2}\pi-\phi_1)$. See Fig. 10. The total energy per unit volume for this type of structure is given by Eq. (13).

The equilibrium conditions $\partial E/\partial\theta_1=0$, $\partial E/\partial\theta_2=0$, $\partial E/\partial\phi_1=0$, and $\partial E/\partial\phi_2=0$ are, as anticipated, satisfied by $\theta_1=\theta_2=\frac{1}{2}\pi$ and $\phi_1=\phi$, $\phi_2=\frac{1}{2}\pi-\phi_1$.

The equations of motion about the equilibrium point

[16] Henceforth, the quantities (ω/γ), M, and H will be expressed in units of $|K_1/M|$.

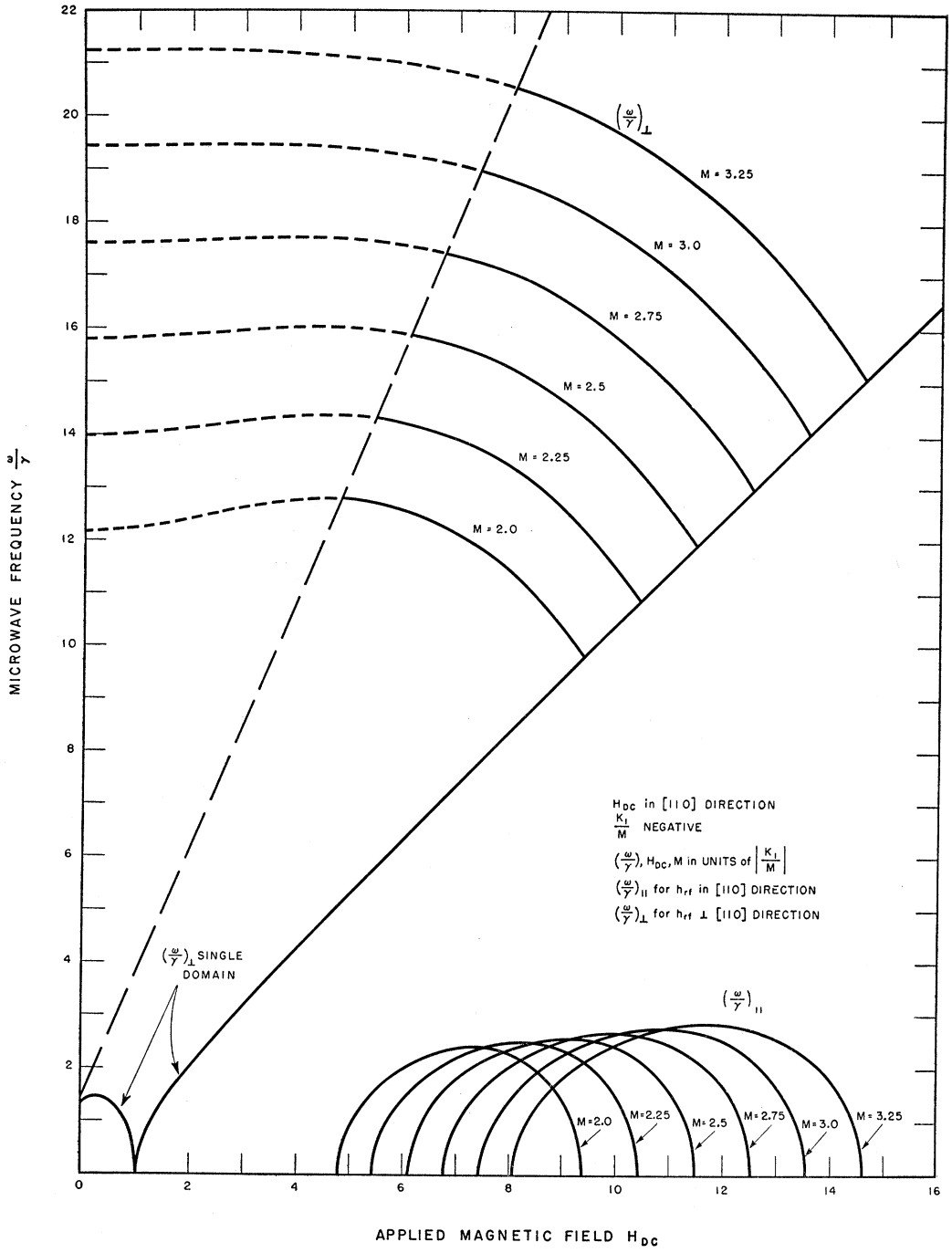

FIG. 9. Resonance relations in cubic crystal; K_1/M negative; **H** in [110] direction.

again yield the two resonance conditions:

$$\left(\frac{\omega}{\gamma}-M\sin\theta\right)_\perp=(AC)^{\frac{1}{2}},\quad \left(\frac{\omega}{\gamma}-M\sin\theta\right)_\parallel=(BD)^{\frac{1}{2}},$$

where A, B, C, and D have been defined previously in terms of the energy derivatives. See Eq. (15).

The expressions for the energy derivatives in this case are:

$$\begin{aligned}
&E_{\theta_1\theta_1}=\tfrac{1}{2}K_1(2-\sin^2 2\phi)+\tfrac{1}{2}MH\sin(\tfrac{1}{4}\pi+\phi)-\tfrac{1}{3}\pi M^2\sin 2\phi,\\
&E_{\theta_1\theta_2}=\tfrac{1}{3}\pi M^2,\\
&E_{\phi_1\phi_1}=K_1\cos 4\phi+\tfrac{1}{2}MH\sin(\tfrac{1}{4}\pi+\phi)\\
&\qquad\qquad -\tfrac{1}{3}\pi M^2\sin 2\phi+\tfrac{1}{2}\pi M^2\sin^2(\tfrac{1}{4}\pi-\phi),\\
&E_{\phi_1\phi_2}=\tfrac{1}{3}\pi M^2\sin 2\phi+\tfrac{1}{2}\pi M^2\sin^2(\tfrac{1}{4}\pi-\phi).
\end{aligned}\qquad (20)$$

Families of the multiple-domain ω/γ *vs* H resonance curves are shown superimposed on the single-domain $\psi=90°$ resonance curve in Fig. 11. M, H, and ω_H/γ are normalized by being expressed in units of K_1/M.

The energy, equilibrium, and resonance relations for the chosen structure are, expressing quantities in units of K_1/M:

$$E=\tfrac{1}{4}(\sin^2 2\phi)-H\sin(\tfrac{1}{4}\pi+\phi)+\tfrac{1}{3}\pi M(1+\sin 2\phi),$$
$$H=\frac{\sin 4\phi+(4/3)\pi M\cos 2\phi}{2\cos(\tfrac{1}{4}\pi+\phi)}, \tag{21}$$

$$(\omega/\gamma)_\perp=\{[2-\sin^2 2\phi+H\sin(\tfrac{1}{4}\pi+\phi)+(4/3)\pi M\sin^2(\tfrac{1}{4}\pi-\phi)][2\cos 4\phi+H\sin(\tfrac{1}{4}\pi+\phi)+4\pi M\sin^2(\tfrac{1}{4}\pi-\phi)]\}^{\frac{1}{2}},$$
$$(\omega/\gamma)_\parallel=\{[2-\sin^2 2\phi+H\sin(\tfrac{1}{4}\pi+\phi)-\tfrac{2}{3}\pi M(1+\sin 2\phi)][2\cos 4\phi+H\sin(\tfrac{1}{4}\pi+\phi)-(4/3)\pi M\sin 2\phi]\}^{\frac{1}{2}}. \tag{22}$$

When observing $(\omega/\gamma)_\perp$ a total of none, one, two, or three resonances may be seen as the dc magnetic field is increased from zero upward. The number of resonances seen depends on the values of (ω/γ) and M. The resonance at the highest field value is the usual single-domain resonance. The $(\omega/\gamma)_\perp$ resonance terminates on the single-domain curve at $H=(4/3)\pi M+2$ at which $\phi=\frac{1}{4}\pi$. Similarly none, one, or two resonances may be seen when investigating $(\omega/\gamma)_\parallel$.

As expected, the total energy for this structure at a given H is never greater than the energy for the single-domain structure.

A "gross susceptibility tensor" χ_g may be defined as in Part *A* of this Section. With reference to the coordinate system used previously, the tensor elements are now:

$$\chi_{g11}=\frac{4\pi M^2 A\sin^2(\tfrac{1}{4}\pi+\phi)}{AC-z^2},$$
$$\chi_{g22}=\frac{4\pi M^2 C}{AC-z^2},$$
$$\chi_{g33}=\frac{4\pi M^2 B\sin^2(\tfrac{1}{4}\pi-\phi)}{BD-z^2},$$
$$\kappa_{g12}=\kappa_{g21}=\kappa_g=\frac{4\pi M^2 z\sin(\tfrac{1}{4}\pi+\phi)}{AC-z^2}, \tag{23}$$

where $z=(\omega-j/T)M/\gamma$ and A, B, C, and D are defined through Eqs. (15) and (20).

V. MAGNETIZATION CURVES PREDICTED FROM POSTULATED MULTIDOMAIN STRUCTURE

The form of the magnetization curves when **H** is applied in a [110] direction follows immediately from the analysis of the previous section. For the negative anisotropy case $H=(3\sin^2\theta-2)\cdot|K_1/M_s|+(4/3)\pi M_s\sin\theta$ and the observed magnetization M_{obs} equals $M_s\sin\theta$. If we write $f=\sin\theta=M_{\text{obs}}/M_s$ and express H and $|K_1/M_s|$ in units of M_s, the following relation is obtained:

$$H=(3f^2-2)f\cdot|K_1/M_s|+(4/3)\pi f, \tag{24}$$

where $1\geq f\geq(\frac{2}{3})^{\frac{1}{2}}$.

Similarly, for positive anisotropy,

$$H=\frac{\sin 4\phi}{2\cos(\tfrac{1}{4}\pi+\phi)}K_1/M_s+(4/3)\pi M_s\frac{\cos 2\phi}{2\cos(\tfrac{1}{4}\pi+\phi)}$$

and

$$M_{\text{obs}}=M_s\sin(\tfrac{1}{4}\pi+\phi).$$

If $g=\sin(\frac{1}{4}\pi+\phi)=M_{\text{obs}}/M_s$, then, in reduced units,

$$H=2g[2g^2-1]\cdot K_1/M+(4/3)\pi g \tag{25}$$

$1\geq g\geq 1/\sqrt{2}$.

These formulas, of course, would not be expected to apply at low magnetic field values at which the simple multidomain structure would not exist. A derivation leading to similar formulae has been given by Bozorth.[17] However, the geometrical shapes of the domains and the domain-wall demagnetization energy factors are not discussed.

VI. COMPARISON OF THEORY WITH RECENT EXPERIMENTAL RESULTS

Detailed investigations on single-crystal ferrites have recently been reported by Tannenwald.[10,11] In his paper on a group of Mn ferrites (crystals with negative anisotropy), Tannenwald[11] states that no combination of K_1/M, K_2/M, and g gave a good fit to the angular variation of resonance field observed. This apparent discrepancy between the calculated angular variation of resonance field and the experimental results can now be removed. For example, the experimental values found for Mn-Zn ferrite at 77°K and 9.198 kMc/sec are shown

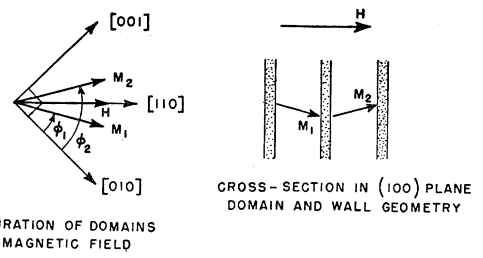

FIG. 10. Multidomain structure in positive anisotropy crystal; **H** in [110] direction.

[17] R. M. Bozorth, *Ferromagnetism* (D. Van Nostrand Company, Inc., New York, 1951), pp. 578–579.

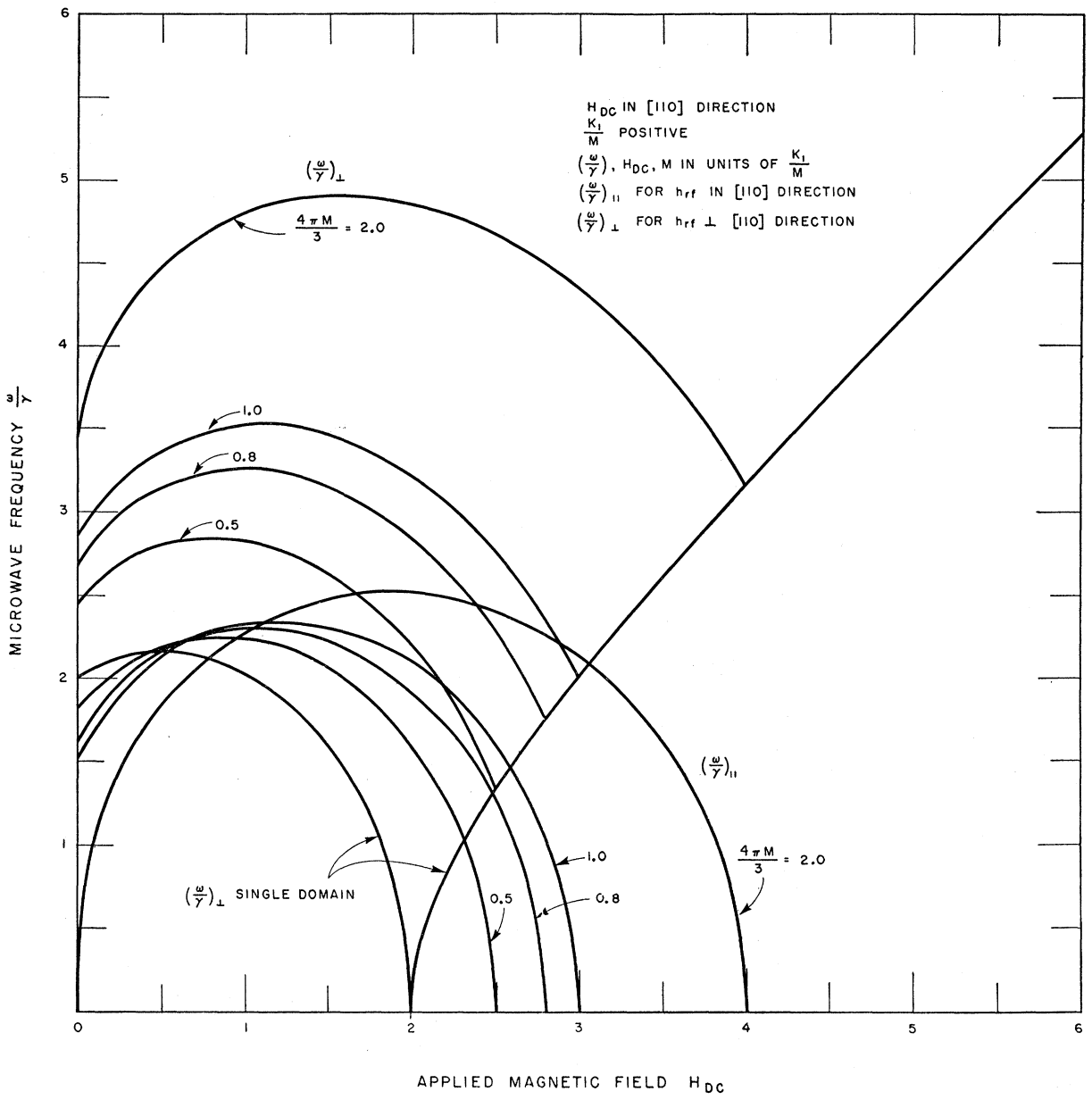

FIG. 11. Resonance relations in cubic crystal; K_1/M positive; **H** in [110] direction.

in Fig. 12.[18] From the field values at 0°, 54°44′, and 90° (4054, 2670, and 3146 oersteds, respectively) the following parameters were computed: $K_1/M = -399$ oe, $K_2/M = -121$ oe, $\omega/\gamma = 3256$ oe. Two curves of resonance field *vs* orientation angle were computed from these data and plotted in Fig. 12. In the first, the magnetization **M** was considered to be parallel to the magnetic field **H**. In the second, the angle between **M** and **H** was taken into account by applying the first order angle correction as given in Eq. (10). As expected, the experimental data lie on the *second* curve.

At a frequency of 9.150 kMc/sec, Tannenwald observed additional ferrite resonances under appropriate temperature conditions. These secondary resonances occurred at magnetic fields below that necessary for the usual resonance. The secondary low-field resonances were not found when the crystal was magnetized in the easy direction; nor were they found at all at 23.0 kMc/sec.

The explanation for these effects is quite direct in terms of the magnetic domain structure discussed in

[18] Data furnished by P. E. Tannenwald (private communication).

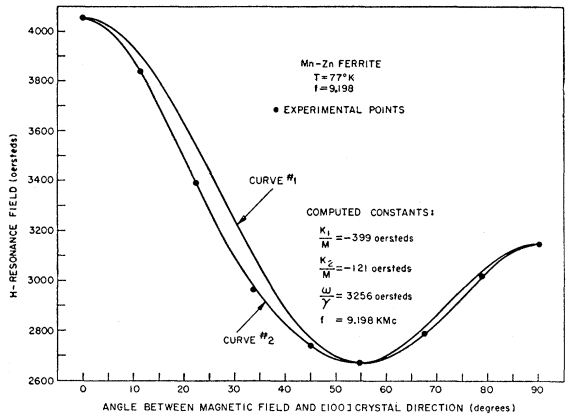

FIG. 12. Variation of resonance field with crystal orientation angle (negative anisotropy crystal).

Sec. IV. 23.0 kMc/sec is apparently too high an operating point for observation of the secondary resonances. No domain structure effects would be expected in the easy crystal direction. The curve relating low-field resonance point to temperature in Mn-Fe ferrite (Fig. 12 in reference 11) is reproducible when one uses Tannenwald's results for K_1/M, the nomogram in Fig. 9, and M values which, for example, range from 591 cgs units at 40°K to 577 cgs units at 138°K. These M values are within the range of values deduced from the magnetization data of Pauthenet[19] and the x-ray density data of Verwey and Heilmann.[20] Although some of these crystal data have been criticized by Gorter,[21] the question is rather moot since magnetic moment and density measurements have *not* been made on the spherical specimen actually used in Tannenwald's microwave experiments. (Variation of properties in different portions of even a given ferrite crystal is quite common.)

The results for positive anisotropy crystals obtained in this paper can be applied to the phenomena observed by Tannenwald in Co ferrite.[10,22] The variation of resonance field with direction (Fig. 4 in reference 10) can be reproduced with fair accuracy using the nomogram of Fig. 4. A better fit should be obtained by considering, in addition, second order anisotropy, but these more general calculations have not been made. An approximate calculation for the angular variation of resonance field was made in the same manner as in the Mn ferrite case discussed previously. The results are shown in Fig. 13.[23] From the three principal direction field values (2850, 9750, and 7700 oersteds) at 90°C and 23.8 kMc/sec the following parameters were computed: $K_1/M=1826$ oersteds, $K_2/M=1830$ oersteds, $\omega/\gamma=6502$ oersteds. The two curves of resonance field *vs* orientation angle computed from these data are plotted in Fig. 13. In the first, **M** was considered as parallel to **H**. In the second, the first order angle correction of Eq. (10) was applied. Some discrepancies still exist between the experimental data and the second curve. This is not too surprising. First, the first order angle correction probably is not adequate. The first order correction is considered adequate for 5° or less but here corrections of as much as 12° were encountered.[24] Secondly, the data are

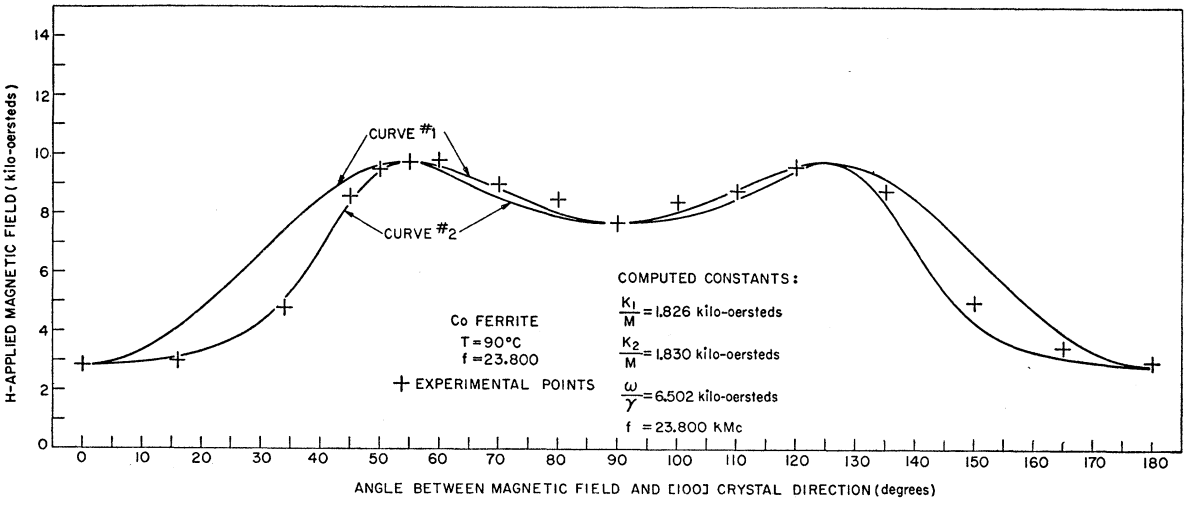

FIG. 13. Variation of resonance field with crystal orientation angle (positive anisotropy crystal).

[19] R. Pauthenet, Compt. rend. **230**, 1842 (1950).
[20] E. J. W. Verwey and E. L. Heilmann, J. Chem. Phys. **15**, 174 (1947).
[21] E. W. Gorter, Philips Research Repts. **9**, 295, 321, 403 (1954).
[22] The parameters and resonance points given by Tannenwald for Co ferrite at 90°C and 23.8 kMc/sec have been recalculated using analyses described in earlier sections. From the hard- and easy-direction resonance point values, one obtains $K_1/M=2070$ oe, $g=2.43$, $(\omega/\gamma)/(K_1/M)=3.37$. Using, in addition, the intermediate axis direction resonance point value, one obtains $K_1/M=1826$ oe, $K_2/M=1830$ oe, $g=2.61$, $\omega/\gamma=6.502$ oe, $(\omega/\gamma)/(K_1/M)=3.56$. These values differ somewhat from those given by Tannenwald.[10]
[23] Experimental data were furnished by P. E. Tannenwald (private communication).
[24] A plot, very much the same as curve 2, can be obtained from the nomogram of Fig. 4. Owing to neglect of second order anisotropy, this curve is raised in the region near 90°.

not internally consistent, since the resonance points do not quite lie on a curve symmetrical about $\theta=90°$. The crystal may be sufficiently misaligned to cause detectable skewness in the observed points.

The secondary peaks observed (Tannenwald's Fig. 3) were, as expected, absent in the easy direction of magnetization. The appearance of the secondary peak in the [110] direction can be understood by referring to the multidomain nomogram of Fig. 11. At a frequency $(\omega/\gamma)/(K_1/M)=3.37$ two secondary peaks would be seen if an $(4/3)\pi M/(K_1/M)$ curve of value 0.9 is intercepted. This apparently is what has happened, the two secondary peaks blending to form a blob. A more detailed comparison is not possible since the Co ferrite resonances are very broad. Moreover, as in the Mn case, data on the magnetic properties of the sample used in the microwave experiments are not available.

We have taken further data on Co ferrite at a frequency of 47.3 kMc/sec at room temperature and at 50°C. At room temperature, K_1/M was 3.6 kilo-oersteds and the g value was 3.3. The resonances were several thousand oersteds in width, making observation difficult. An indication of multiple-domain effects was seen.

Low-field resonances have been seen also by Hubbard in Ni ferrite[13] and White and Solt in Co ferrite,[12] but their data are at present only preliminary.

Smit and Beljers[2] have reported observations of $(\omega/\gamma)_{\parallel}$ in a uniaxial crystal. Observations of $(\omega/\gamma)_{\parallel}$ on cubic ferrites apparently have not yet been made.

VII. ACKNOWLEDGMENTS

The computations were performed by Mrs. Marjorie M. Campbell and W. D. Doyle of Lincoln Laboratory, and also by the Parke Mathematical Laboratory. The author is indebted to his former colleagues, P. E. Tannenwald and S. Foner, for many valuable discussions.

APPENDIX—EQUILIBRIUM AND RESONANCE RELATIONS IN PRESENCE OF MAGNETIC DOMAIN STRUCTURE

A. Negative Anisotropy Crystals—H in [110] Direction

Three types of the lamellar domain structure such as that described in Sec. V were considered. Each corresponded to magnetizations lying in the (110) plane tilted equally with respect to the [110] direction. The model finally adopted had the domain walls oriented perpendicularly to the dc magnetic field. The energy per unit volume in this arrangement was given in Eq. (13). The alternative structures differed in the orientation of the domain walls. In the first alternative the domain walls were parallel to $\mathbf{H}_{dc}$ and perpendicular to the [100] direction. In the second the walls were parallel to $\mathbf{H}_{dc}$ and parallel to the (110) plane. The domain energy term of the first model,

$$\tfrac{1}{2}\pi M^2[\sin\theta_1\cos(\tfrac{1}{4}\pi-\phi_1)-\sin\theta_2\cos(\tfrac{1}{4}\pi-\phi_2)]^2,$$

is replaced by

$$\tfrac{1}{2}\pi M^2(\cos\theta_1-\cos\theta_2)^2$$

and

$$\tfrac{1}{2}\pi M^2[\sin\theta_1\cos(\tfrac{1}{4}\pi+\phi_1)-\sin\theta_2\cos(\tfrac{1}{4}\pi+\phi_2)]^2,$$

respectively, for consideration of these alternative models. At the equilibrium point $\theta=\theta_1=\pi-\theta_2$, $\phi_2=\phi_1=\frac{1}{4}\pi$, the domain energy term for the first alternative model has a positive value $2\pi M^2\cos^2\theta$, whereas the corresponding term for the other two models is zero. Hence, this model was not considered further. The second alternative yielded solutions in which the $(\omega/\gamma)_{\perp}$ curve sloped upward to the right as H was increased. Only *one* resonance would have been seen in this case. Hence, this alternative was also discarded.

B. Positive Anisotropy Crystals—H in [110] Direction

As in the negative anisotropy case, three types of lamellar domain structures were considered. Each corresponded to magnetization lying in the (100) plane tilted equally with respect to the [110] direction. The model finally chosen (as in the negative anisotropy analysis) had the domain walls oriented normally to the dc magnetic field. The energy per unit volume for this model (as given in Eq. (13)) included a domain energy term

$$\tfrac{1}{2}\pi M^2[\sin\theta_1\cos(\tfrac{1}{4}\pi-\phi_1)-\sin\theta_2\cos(\tfrac{1}{4}\pi-\phi_2)]^2.$$

At equilibrium, $\theta_1=\theta_2=\frac{1}{2}\pi$, $\phi=\phi_1=\frac{1}{2}\pi-\phi_2$, this domain energy term is zero.

The two alternative structures corresponded to walls oriented parallel to the dc field. The first alternative examined had walls in the (110) plane with the domain energy

$$\tfrac{1}{2}\pi M^2[\sin\theta_1\sin(\tfrac{1}{4}\pi-\phi_1)-\sin\theta_2\sin(\tfrac{1}{4}\pi-\phi_2)]^2.$$

This domain energy gives a positive contribution at equilibrium. Hence, this model was discarded.

The second alternative had a structure composed of walls in the (100) plane. The domain energy was $\frac{1}{2}\pi M^2(\cos\theta_1-\cos\theta_2)^2$. This formulation yielded the identical equilibrium condition as the finally adopted case. However, the $(\omega/\gamma)_{\perp}$ curve in this instance was below the $(\omega/\gamma)_{\perp}$ curve of the first model and did not correspond to available experimental data. This model also was not considered further.